JOURNAL OF MATERIALS SCIENCE 9 (1974) 1483–1492

The nature of inclusions in heavily tellurium-doped gallium arsenide

P. W. HUTCHINSON
Department of Physical Metallurgy and Science of Materials, University of Birmingham, Birmingham, UK

B. D. BASTOW
Corrosion and Protection Centre, University of Manchester Institute of Science and Technology, Manchester, UK

Large elongated inclusions in heavily Te-doped ⟨001⟩ Czochralski pulled, GaAs crystals have been studied by a combination of scanning and transmission electron microscopy, electron microprobe analysis and X-ray topography. They have been shown to lie along the ⟨110⟩ directions in the {001} growth plane and to consist of two parts, an outer single crystal region of varying composition based on Ga_2Te_3 and an inner polycrystalline core rich in Te and As. Their crystallography has been interpreted in terms of impurity segregation and facet formation during crystal growth while their composition is discussed with reference to the Ga–As–Te phase diagram.

1. Introduction

Interest in Te-doped GaAs arises from its usefulness in the preparation of electroluminescent diodes and semiconductor injection lasers and a detailed knowledge of the defect population and impurity distribution is important both in interpreting device characteristics and in materials selection.

Inhomogeneities in Te-doped GaAs have been investigated previously by a number of workers using autoradiography [1], electron microprobe analysis [2] and X-ray topography [3], Casey [4] has suggested that the observed impurity striations may be due to a non-uniform distribution of a Te-rich phase or complex and that this Te enriched zone could be associated with the difference between the Te concentration and the carrier concentration observed in other studies of this material [1, 2].

Previous work on the defect structure of GaAs has revealed the presence of both precipitates and stacking fault complexes. Meieran [5] and Laister and Jenkins [6] both observed stacking faults in melt grown Te-doped GaAs with carrier concentrations, N, greater than 1×10^{18} cm^{-3}. Since the number of stacking faults increased with Te concentration, Laister and Jenkins suggested that the faults were formed by the aggregation of Te atoms on {111} planes to form extrinsic faults. Comparison with the results of Abrahams *et al.* [7] for Se-doped GaAs suggests that these faults may correspond to Ga_2Te_3 precipitates. Te-rich microprecipitates have also been observed by Meieran [5] and Iizuka [3] for carrier concentrations greater than 1×10^{18} cm^{-3}.

Much larger precipitates have been observed by Iizuka [8] in (111) slices of boat grown Te-doped GaAs with $N = 6.8 \times 10^{18}$ cm^{-3}.These triangular inclusions were observed on the As (111) face and consisted of a Ga–Te complex with a very low As concentration. Occasionally a reverse pointed triangle surrounding these inclusions was also seen. The latter region contained approximately equal amounts of As and Ga and the Te concentration was much higher than in the host GaAs matrix.

The present paper describes an investigation of inclusions found in Te-doped GaAs carried out as part of a study of the defect structure of GaAs. The precipitates have been examined using scanning electron microscopy (SEM) transmission electron microscopy (TEM), electron microprobe analysis (EMPA) and X-ray topography (XRT). A number of interesting structural details have been observed and the precipitate morphology has been interpreted in terms of faceted growth of the host GaAs

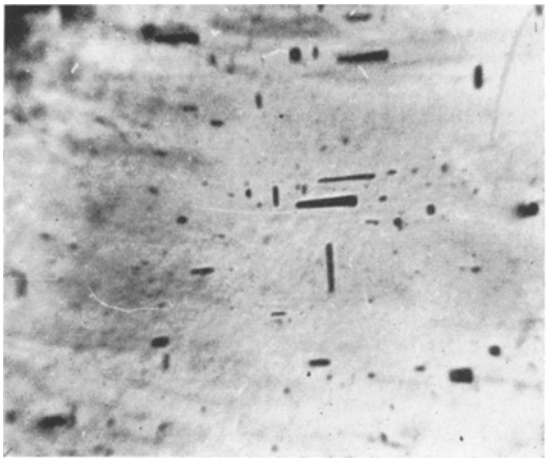

Figure 1 The volume distribution of inclusions in a GaAs (001) slice, 1000 μm thick and their variation in size and shape. Transmission infra-red image (× 15).

crystal. An attempt has been made to interpret the composition of the precipitates in terms of the Ga–As–Te phase diagram.

2. Experimental techniques

Slices of GaAs were cut normal to the growth direction of [001] pulled, liquid encapsulated, Czochralski grown single crystals. Specimens for examination were selected from various parts of the ingots. The carrier concentration of the lightly doped slices was 4×10^{17} cm^{-3} while that of the tail-end slices contained between 6×10^{18} and 8.4×10^{18} carriers cm^{-3}. It is noted that since the true Te concentration may be larger than the measured carrier concentration [1, 2] the dopant levels given in the present paper in terms of N may only be minimum values and the true Te concentrations may be significantly larger.

The slices were mechanically polished using diamond impregnated cloths and any residual surface damage was removed with a chemical-mechanical polish using a 3% bromine-methyl alcohol solution [9]. The depth distribution of precipitates in the slices was revealed by infra-red microscopy (Fig. 1) and polishing was continued until a precipitate was exposed on the surface. The slices were also examined by transmission XRT using a Jarrall-Ash Model 80-050 Lang Camera to determine the general distribution of precipitates and the segregation pattern.

The exposed precipitates were examined by SEM using a Cambridge Stereoscan in the d.c. back scattered mode in order to obtain electron channelling patterns to determine the precipitate orientations.

Analysis of the precipitates was carried out on a Cambridge Microscan Mark V microanalyser using an accelerating voltage of 25 kV. Spot counts were made at fixed intervals across the precipitates for all three components. Undoped GaAs ($N \sim 1 \times 10^{16}$ cm^{-3}, i.e. 0.5 ppm) and Johnson-Matthey Te (< 5 ppm impurities) were used as standards. Counting rates were kept low enough to minimize dead-time corrections while counting for sufficient time to give less than 1% counting error.

Specimens for examination by TEM in an AEI EM6G microscope were prepared by ultrasonically cutting 3 mm diameter discs from the slices and thinning was carried out using either a chemical etching technique [10] or in an Edwards ion beam machining instrument. While the chemical method was suitable for thinning homogeneous GaAs, preferential dissolution of the precipitates can occur and the ion beam method was obligatory for thinning the precipitates themselves.

3. Results and interpretation

3.1. General characteristics

Large, elongated inclusions were observed intersecting the polished (001) surfaces of slices with $N \geqslant 7.4 \times 10^{18}$ cm^{-3} taken from the extreme tail end of the Te-doped GaAs ingots. Similar features were never observed in less heavily Te-doped specimens or in GaAs doped with Si and Se up to concentrations of 4×10^{18} cm^{-3}. In particular the maximum doping level of Se was higher than in the bulk samples examined by Abrahams *et al.* [7] and no inclusions were observed in the present investigation. The absence of inclusions in GaAs containing other dopants may be because the partition coefficient for Te is unusually low; $k_0 = 0.059$ [11]. This results in a very large rejection of Te into the melt during solidification of the GaAs. Also in order to prepare material with high Te levels the melt must be relatively rich in Te. In the case of other dopants where the partition coefficients are larger the melt need not be as heavily doped and there is less rejection of the dopant into the melt. Consequently, there is less chance of the formation of inclusions rich in the dopant. The number of inclusions in the Te-doped GaAs increased as the extreme tail end of the crystal was approached.

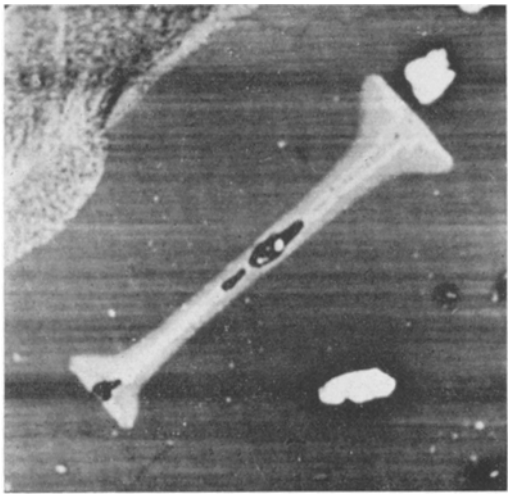

Figure 2 Specimen current image of inclusions (× 80) obtained using EMPA showing signs of faceted growth.

The exposed inclusions were often sufficiently large to be seen by the naked eye though they varied considerably in size. Typical dimensions were about 500 μm long and 50 μm wide. Most of the inclusions were "bone shaped" as shown in Fig. 2 though some were rectangular (Fig. 1). Repeated polishing and examination indicated that they were also approximately 50 μm thick and were not elongated in the crystal growth direction. A section through a precipitate obtained by cleavage of a (100) slice on a {110} plane followed by polishing and etching in a 3% bromine-methyl alcohol solution is shown in Fig. 3a. The section is triangular and there are signs of faceting along the interface across the middle of the precipitate as noted in the interpretation of the section in Fig. 3b. While this triangular cross-section was observed in a number of cases other, often irregular, shapes were also noted.

3.2. Crystallography

The orientation of the precipitates with respect to the GaAs matrix was determined from the GaAs electron channelling pattern obtained using SEM. Fig. 4 clearly indicates that the precipitates are aligned parallel to the ⟨110⟩ directions and perpendicular to the [001] growth axis.

Transmission XRT of heavily doped slices also revealed distinctive features with the same orientation. Fig 5a shows the topograph, obtained using the 040 reflection, of a slice containing 8.4 × 10^{18} carriers cm^{-3} taken from

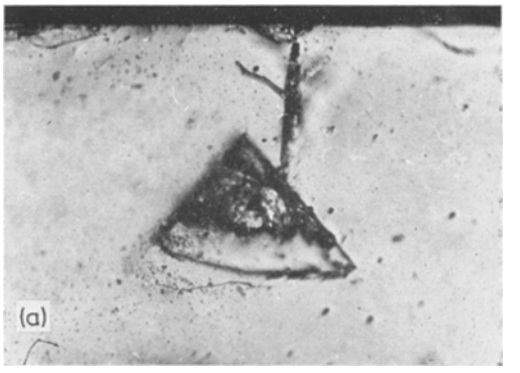

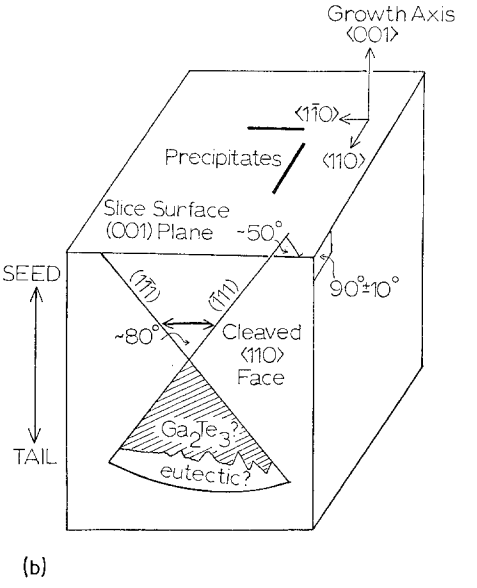

Figure 3 (a) Cross-section through on inclusion approximately on the (110) plane showing signs of faceted growth at the interface between the two parts of the inclusion (× 51). (b) Relation of the inclusion cross section to the orientation of the GaAs matrix.

the same ingot as the slice shown in Fig. 4. Large, elongated, rectangular features ~ 250 μm wide and 2000 μm long are seen lying along the ⟨110⟩ directions. Fig. 5b shows a topograph of a slice with a smaller carrier concentration (N = 6.5 × 10^{18} cm^{-3}) where the marked crystallographic orientation of the striations has disappeared and only an irregular wavy pattern remains. Similar wavy patterns were observed by infra-red microscopy. No discrete precipitates were observed in this slice. A slice from the same ingot containing 7.4 × 10^{18} carriers cm^{-3} produced a topograph showing both aligned and wavy features which indicates that this is close to the critical concentration for the alignment

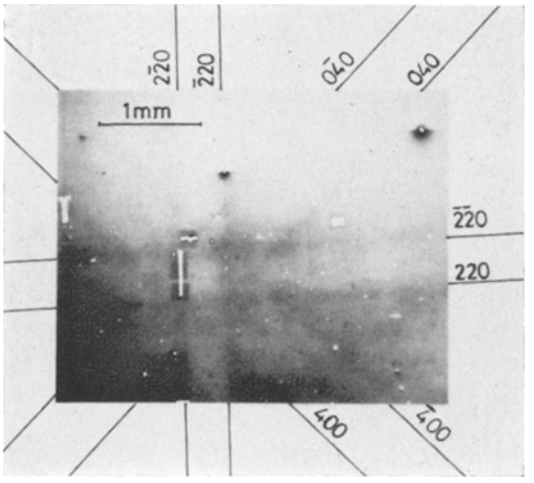

Figure 4 Orientation dependent electron channelling pattern obtained by SEM showing the (001) pole and inclusions parallel to the ⟨110⟩ directions (× 13.5). Carrier concentration = 7.4 × 10^{18} cm^{-3}.

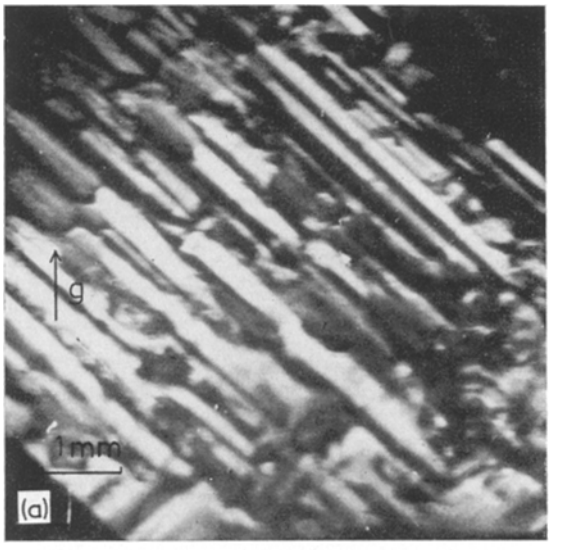

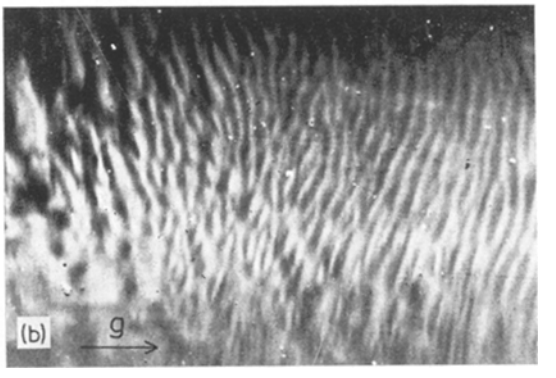

Figure 5 X-ray transmission topographs of GaAs taken with Mo$K\alpha$ radiation $\mu_L t$ = 10. (a) N = 8.4 × 10^{18} carriers cm^{-3}. The operating reflection, $\boldsymbol{g}$ = 040, is perpendicular to the ⟨001⟩ crystal growth direction which points out of the plane of the paper (× 10.5). (b) N = 6.5 × 10^{18} carriers cm^{-3}. The operating reflection $\boldsymbol{g}$ = 220 (× 10.5).

of striations along crystallographic directions. The change in the nature and alignment of these features as the tail is approached is shown schematically in Fig. 6. Similar features were never observed in slices doped less heavily than 7 × 10^{18} cm^{-3} with Te or doped with other impurities.

Although the inclusions (Fig. 4) and the striations (Fig. 5) have the same orientation which suggests that they are related phenomena the precipitate and striation densities are not comparable. This suggests that the striations are merely a segregation effect which only becomes large enough to lead to precipitation at a few places where liquid rich in Te accumulates as described below.

3.2.1. Faceted growth mechanism

The shape and orientation of the inclusions and striations can be explained by assuming that constitutional supercooling and faceting occur during crystal growth. As growth proceeds the concentration of Te in the melt increases since the partition coefficient is very small and the tail end of a pulled crystal is produced from a melt rich in Te. If constitutional supercooling occurs impurity segregation causing striations similar to those shown in Fig. 5b may be produced. Work by Morizane *et al.* [12] has shown that similar striations in InSb are caused by temperature fluctuations at the solid-liquid interface due to sharp temperature gradients in the growing crystal near the interface. At the extreme end of the crystal the pulling rate is increased in order to terminate growth and this will further enhance constitutional supercooling and could lead to facet formation on the advancing solid interface. Cronin *et al.* [1] have, in fact, found evidence of faceting on {111} planes during the growth of Te-doped GaAs and have detected differences in Te concentrations between faceted and unfaceted regions. The evidence from XRT (Fig. 5) indicates that the segregation pattern is initially random but becomes oriented as the tail end is approached and finally becomes faceted and associated with inclusions. At this point the

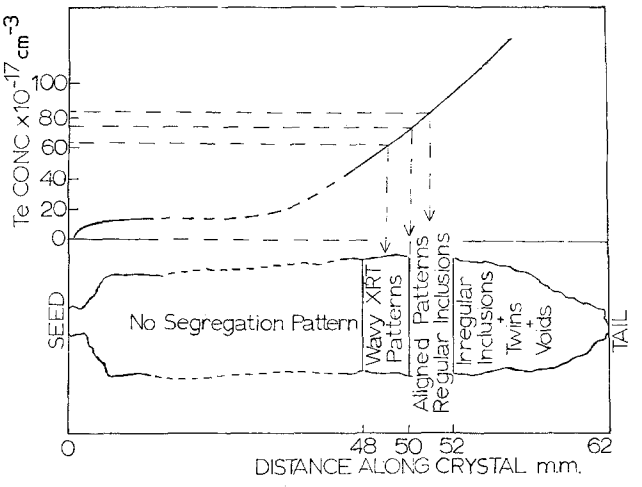

Figure 6 Relative positions of observed features and their relation to the approximate doping levels.

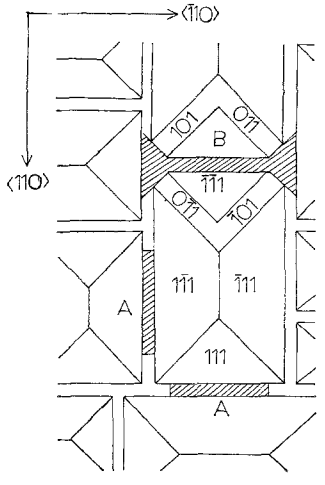

Figure 7 Schematic plan of solid-liquid (001) interface showing faceting on {111} and {110} planes and the formation of rectangular (A) and "bone shaped" (B) inclusions.

(001) solid-liquid interface may consist of pyramidal cells with {111} facets similar to those described for germanium by Bardsley *et al.* [13] and shown schematically in Fig. 7.

If the rate of growth of the facets is fast enough (which is most probable when the pulling rate is increased at the end of the ingot) and if the Te-rich liquid segregating at the interface remains liquid well below the freezing point of GaAs (1238°C) then the liquid will become trapped in channels lying along ⟨110⟩ directions and will be incorporated into the GaAs crystal. This mechanism is also consistent with the shape of the inclusion cross-section shown in Fig. 3 where the liquid forming the inclusion is trapped between two planes which form an angle of ~ 80° which is close to that between {111} planes intersecting a {110} plane (70°54′). The liquid inclusion appears to have been held in the channel by surface tension forces until it has been enclosed by GaAs. The subsequent solidification of this liquid will then produce rectangular inclusions in the observed orientation as shown at A in Fig. 7. The distinctive triangular shape of the ends of many of the inclusions may arise because of secondary faceting along {110} planes as shown at B since the angles between the ⟨110⟩ and diagonal edges is approximately 45°.

The formation of the triangular inclusions observed by Iizuka [8] may possibly be explained by a similar mechanism. The formation of {111} facets on a {111} growth interface could produce tetrahedral cavities filled with Te-rich liquid. Sections in the (111) plane through the inclusion formed from this liquid would be equilateral triangles with edges parallel to the ⟨110⟩ directions. Unfortunately, Iizuka gives insufficient crystallographic information to determine whether this interpretation is correct.

3.3. Composition of phases

The X-ray images shown in Fig. 8 clearly reveal that the inclusion consists of two distinct regions, both rich in Te. The Ga$K\alpha$ image shows signs of crystallographic growth facets similar to those seen in Fig. 2. The electron image also indicates that the central section is associated with a

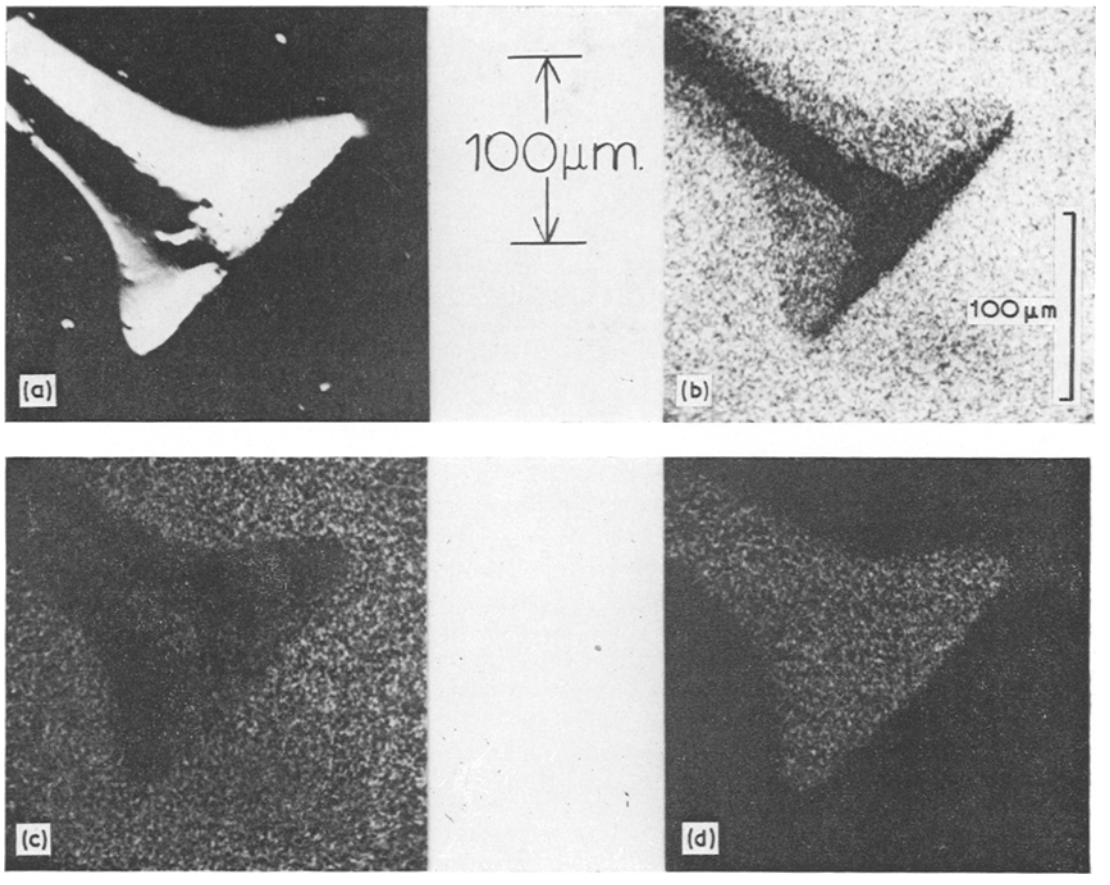

Figure 8 Electron and X-ray images of an inclusion (a) electron image (b) Ga$K\alpha$ (c) As$K\alpha$ (d) Te$L\alpha$. In the X-ray images the brightness of the picture increases with the concentration of the relevant element. The brightness of the background in (b) and (c) corresponds to $\sim$ 50 wt % Ga and As respectively ($\times$ 240).

relief effect. This could not be removed by light polishing, possibly because of the very loose and friable nature of the core. The effect clearly creates difficulties in obtaining completely reliable quantitative analysis but while there is some scatter in the spot counting results shown in Fig. 9 in the central region the two regions can be readily associated with specific sections of the profiles. The wt % compositions of the two-regions were obtained from the relevant parts of the profiles by correcting the K_A values plotted in Fig. 9 using a well established procedure [14].

The composition of the inclusion core corresponds to the empirical formula $Ga_7As_{35}Te_{58}$ and may possibly be a solid solution of Ga in As_2Te_3 although the constant composition may also be evidence of a eutectic composition, as discussed in Section 3.5. The outer shell has a continuous composition variation across it corresponding to a change from $Ga_{40}As_{20}Te_{40}$ to $Ga_{35}As_6Te_{59}$. These very approximate formulae suggest that this region is a solid solution based on Ga_2Te_3 with As substituting for Te. Solid solutions of As in Ga_2Te_3 have been reported previously by Woolley and Smith [15] who noted that equilibrium in these solid solutions was only reached very slowly which may explain why the non-uniform composition produced on solidification has not annealed out.

Iizuka [8] has also qualitatively analysed triangular inclusions in Te-doped GaAs and while no compositions are given it appears from a comparison of the relative intensities of the X-ray images with those in Fig. 8 that they also correspond to a solid solution of As in Ga_2Te_3. He also observed an outer region richer in Te but with Ga and As concentrations very close to those of the matrix. This appears to be GaAs very heavily doped with Te but no evidence for a similar region was found in the present work.

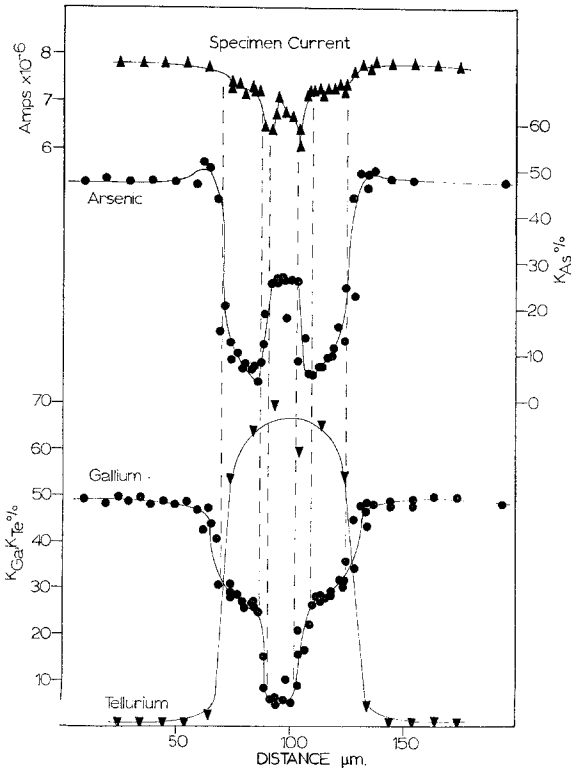

Figure 9 Concentration profiles across a precipitate.

Iizuka did not report any evidence for an As enriched core region similar to the one described above. However, the observed distribution of the elements may be largely dependent on the section of the inclusion examined. While the cross-section shown in Fig. 3 suggests that the Ga_2Te_3 and As_2Te_3 regions are separated, a section a few hundred microns further along suggests that the lighter (As_2Te_3?) region becomes completely enclosed by the darker phase. Similarly X-ray images of other inclusions show Ga rich regions at each end of the core in contrast to the example shown in Fig. 8 where the core is As-rich throughout the length.

3.4. Internal microstructure

Examination by SEM revealed that the core of the inclusion consisted of a cavity incompletely filled with numerous small crystals and that there was considerable micro-porosity. The polycrystalline nature was confirmed by the complex, spotty ring diffraction patterns obtained from this region by TEM (Fig. 10c). An analysis of the pattern was not possible since only a few of the inner rings could be measured even approximately because of their diffuse nature. The multiplicity of spots and *d*-spacings may in fact arise from overlapping rings of three separate phases in a eutectic mixture (see Section 3.5). Great difficulty was experienced in preparing thin foils of this region because of its porous and fragile nature and while some specimens were obtained by ion beam thinning the core region invariably collapsed either during thinning or on examination by TEM when it disintegrated rapidly under the impact of the focused electron beam.

The diffraction pattern obtained from the outer region (Fig. 10a) indicated that this was a single crystal which had grown epitaxially on the cavity walls since the diffraction pattern is not rotated from that of the GaAs matrix. Some evidence of crystallographic growth is also seen in Figs. 2, 3 and 8. The pattern suggests that the structure is similar to that of GaAs but it is complicated by the doubling of many of the spots which introduces difficulties in estimating a lattice parameter for this phase although it is possible to say that the value is larger than that of GaAs. This is consistent with the work of Woolley and Smith [15] and Panish [16] which showed that the lattice parameter of the solid solution based on Ga_2Te_3 had a value of $a > 5.73$ Å while for GaAs $a = 5.653$ Å.

The micrograph of the outer region shown in Fig. 10b clearly indicates that there is a high defect concentration associated with the growth of the single crystal region. This may arise because of the differential thermal contraction between the GaAs and Ga_2Te_3 which creates large stresses in the outer region. Alternatively, the varying composition across the Ga_2Te_3 layer may arise because of diffusion and this will be associated with the generation of further defects. Finally, there will be stresses associated with epitaxial growth and the variation of the lattice parameter from 5.653 Å at the GaAs interface to approximately 5.88 Å [15] at the inner surface.

Since the diffraction pattern from the outer region is similar to that for GaAs, if it is indexed accordingly the defects appear to lie within about 5° of the $[\bar{1}10]$ direction. Since they intersect the specimen surface and do not show any fringe contrast on tilting, the most probable interpretation is that they are dislocations lying along the $[\bar{1}10]$ direction.

TEM of the parent GaAs crystal revealed extrinsic stacking faults identical to those

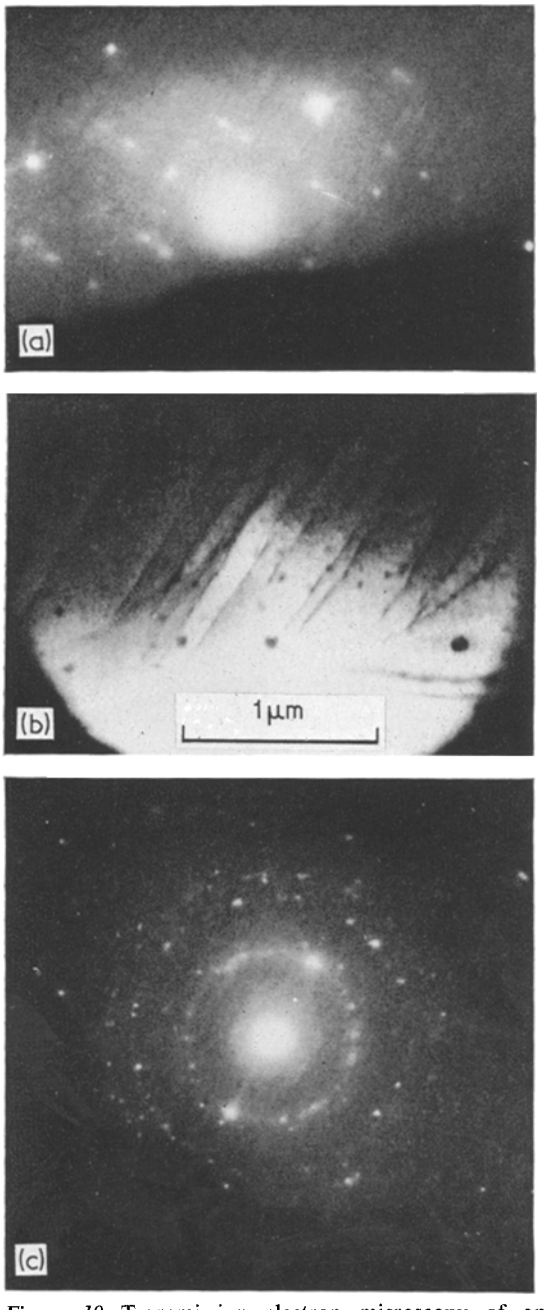

Figure 10 Transmission electron microscopy of an inclusion (a) SAD pattern from the outer region of the inclusion, (b) micrograph of the outer region of inclusion, (c) complex SAD pattern from core of the inclusion from which a micrograph could not be obtained (see Section 3.4).

observed by Laister and Jenkins [6] who interpreted their observations in terms of Te substituting for As on {1 1 1} planes.

3.5. Solidification paths of the entrapped liquid

The estimated compositions of the solid phases are shown in Fig. 11 together with relevant details from the ternary phase diagram [16].

Since the composition range for the Ga_2Te_3 solid solution lies close to the GaAs–Ga_2Te_3 pseudo-binary system it is probably valid to interpret the solidification of this phase in terms of the peritectic reaction in this system at $\sim$ 860°C. As the trapped liquid cools below 1238°C, GaAs is deposited on the walls of the cavity until the peritectic at $\sim$ 860°C is reached when the reaction:

GaAs + liquid $\rightarrow$ G $_2Te_3$ (As in solution)

occurs. The reaction proceeds by the rapid diffusion of As into the liquid and the counter-current diffusion of Te into the GaAs while the outward flow of Ga is much slower. This results in the experimentally observed profiles in the outer region and the production of defects (Fig. 10b). This mechanism also implies that the outer layers of the Ga_2Te_3 solid solution are grown by diffusion in the GaAs matrix and there will be no misorientation between the two phases, in agreement with the TEM results.

The net result of this reaction is that the remaining liquid is enriched in As. Unfortunately, it is not clear from the partial phase diagram given by Panish or from the very approximate liquid compositions estimated from the present analysis exactly how the liquid composition changes during the deposition of the solid solution or on subsequent cooling. Nor is it possible to determine the phases which may be precipitated during this stage. However, from the X-ray diffraction data summarized by Panish it appears that a solid solution based on Ga_2Te_3 can still be formed in alloys corresponding to the composition $Ga_{10}As_{42}Te_{48}$ in the GaAs–Ga_2Te_3 pseudo-binary system. Hence it may be possible that as the liquid composition follows a path down the liquidus surface to the As–Te side of the system the Ga_2Te_3 based solid solution either continues to be formed by the peritectic reaction described above or by direct precipitation from the liquid. For the former case to apply, the liquid composition must follow the locus of the intersection of the liquidus surface and the peritectic plane but the range of composition of the solid solution is not entirely consistent with this path being followed for a major part of its length. Alternatively, and more consistent with the composition range

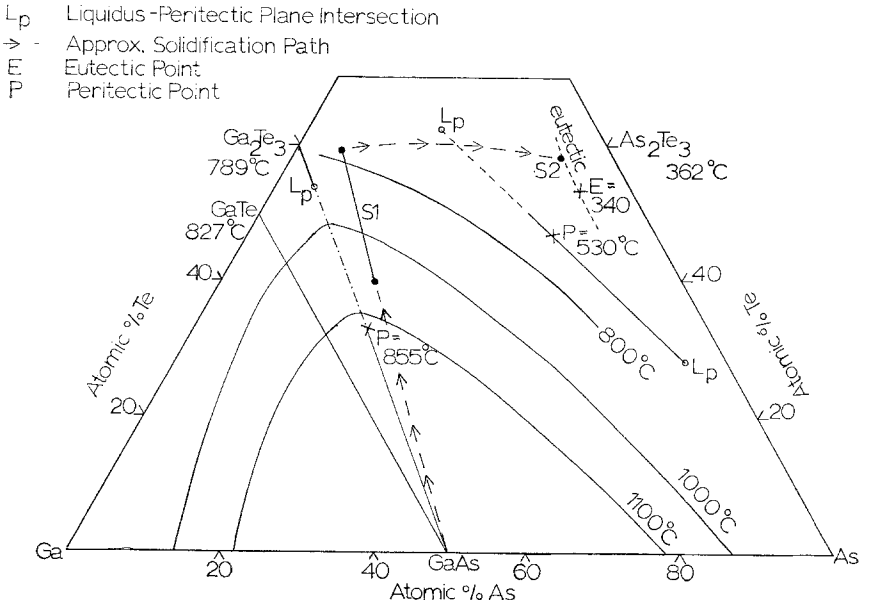

Figure 11 Ga–As–Te phase diagram after Panish [16] showing details relevant to the solidification of Te-rich liquid (see Section 3.5 for details).

given above, direct precipitation occurs, apparently epitaxially, and the growth appears to be faceted (Figs. 2, 3 and 8).

Whichever of these two reactions is the major contributor to the formation of the solid solution, the final result is that the remaining liquid has a composition close to the As–Te binary. The composition of the core region corresponds to the formula $Ga_7As_{35}Te_{58}$ which could be interpreted as a ternary compound based on As_2Te_3. However, there is no published evidence for the solubility of Ga in As_2Te_3 up to 7 at. % Ga. Also an alloy examined by Panish close to the composition contained three phases, Ga_2Te_3, As_2Te_3 and As, and as shown in Fig. 11, there is possibly a eutectic trough very close to S2. The observed constant composition is thought to be due to the liquid composition reaching this eutectic and following it to an invariant ternary eutectic temperature where the remaining liquid solidifies to give a ternery eutectic mixture with a constant average composition. This is also consistent with the complex diffraction pattern from the core region which suggests that more than one phase may be present.

However, while this scheme explains the observed sequence of phases it is emphasized that much of it is speculative because of lack of information in the relevant regions of the ternary phase diagram.

3.6. Relationship between large precipitates and other defects

Casey [4] concluded from an investigation of cathodoluminescence centres in Te-doped GaAs that the observed difference between the total Te concentration and the carrier concentration [1, 2] was associated with the non-uniform distribution of a Te-rich complex or phase. It was considered that this phase was probably a Te-rich ternary solid solution with a crystal structure different from that of GaAs and that it must grow either by rapid diffusion of an unspecified species or by growth into the crystal in order to explain its size. The present work suggests that the properties attributed to this complex are consistent with the solid solution based on Ga_2Te_3 which can be grown into the crystal as large precipitates in some cases if a Te-rich liquid is produced during solidification. However, the crystal structure is the same as that of GaAs although the lattice parameter is slightly larger.

The small precipitates and stacking faults observed by Meieran [5] and Laister and Jenkins [6] may also be possibly explained by the aggregation of Te on As sites. When the GaAs matrix becomes supersaturated with Te in certain regions because of fluctuations in growth conditions a new equilibrium situation can be achieved by the grouping of Te on neighbouring

sites on the As sub-lattice. Laister and Jenkins have suggested that the faults are caused by the substitution of Te for As in one close packed layer and have shown that the stacking faults are associated with a high Te concentration ($N > 10^{18}$ cm^{-3}). Further indirect evidence obtained from electron irradiation studies has also indicated that the faulted layers may contain Te [17]. When the fraction of As sites occupied by Te atoms reaches a critical level an independent stable structure is formed corresponding to the As-rich end of the Ga_2Te_3 based solid solution region. Also since the structures of the GaAs matrix and the precipitate are the same and have similar lattice parameters the coherency strains at the interface will only be small and will not tend to inhibit the formation of these small complexes unduly.

4. Conclusions

In GaAs heavily doped with Te, segregation patterns can be formed, the patterns becoming more regular and oriented in crystallographic directions as the Te concentration increases. The transition from irregular to oriented patterns occurs at a carrier concentration of $\sim 7 \times 10^{18}$ cm^{-3}. At very high Te levels Te-rich liquid can become trapped along channels along $\langle 1\,1\,0 \rangle$ directions in the parent GaAs crystal. The channels are probably formed by faceted growth of the GaAs on $\{1\,1\,1\}$ planes with some secondary faceting on $\{1\,1\,0\}$ planes.

The trapped liquid takes part in a peritectic reaction with the GaAs to give a solid solution based on Ga_2Te_3 and more Ga_2Te_3 precipitates on cooling below the peritectic temperature, probably epitaxially and with faceted growth. This solid solution single crystal based on Ga_2Te_3 but with As substituting for Te has a wide composition range and contains a large number of aligned defects. The remaining liquid solidifies at an invariant temperature to give a polycrystalline, porous region with a constant composition. The small precipitates and stacking fault complexes observed by other workers may be based on the Ga_2Te_3 solid solution.

Acknowledgements

This work was financially supported by a Co-ordination of Valve Development contract and by a Science Research Council grant. We are grateful to Professor R. E. Smallman and Dr P. S. Dobson of the University of Birmingham and Dr J. D. Filby of the Royal Radar Establishment, Malvern for the provision of research facilities. We would also like to thank Dr C. W. Haworth and Mr T. C. Hopkins of the Department of Metallurgy, University of Sheffield for the provision and operation of the microprobe analyser facilities.

References

1. G. R. CRONIN, G. B. LARRABEE and J. F. OSBORNE, *J. Electrochem. Soc.* **113** (1966) 292.
2. D. B. WITTRY, *Appl. Phys. Letters* **8** (1966) 142.
3. T. IIZUKA, *Jap J. Appl. Phys.* **7** (1968) 490.
4. H. C. CASEY, *J. Electrochem. Soc.* **114** (1967) 153.
5. E. S. MEIERAN, *J. Appl Phys.* **36** (1965) 2544.
6. D. LAISTER and G. M. JENKINS, *J. Mater. Sci.* **3** (1968) 584.
7. M. S. ABRAHAMS, C. J. BUIOCCHI and J. J. TIETJEN, *J. Appl. Phys.* **38** (1967) 760.
8. T. IIZUKA, *Jap. J. Appl. Phys.* **7** (1968) 485.
9. M. V. SULLIVAN and G. A. KOLB, *J. Electrochem. Soc.* **110** (1963) 585.
10. C. J. BUIOCCHI, *J. Appl. Phys.* **38** (1967) 1960.
11. R. K. WILLARDSON and W. P. ALLRED, Proceedings of the International Symposium on GaAs, Reading 1966 (Institute of Physic, London, 1967) p. 35.
12. K. MORIZANE, A. F. WITT and H. C. GATOS, *J. Electrochem. Soc.* **113** (1966) 51.
13. W. BARDSLEY, J. S. BOULTON and D. T. J. HURLE, *Solid State Electronics* **5** (1962) 395.
14. T. C. HOPKINS and B. D. BASTOW, *J. Phys. D:Appl. Phys.* **7** (1974) 199.
15. J. C. WOOLLEY and B. A. SMITH, *Proc. Phys. Soc.* **72** (1958) 867.
16. M. B. PANISH, *J. Electrochem. Soc.* **114** (1967) 91.
17. P. W. HUTCHINSON and P. S. DOBSON, to be published in *Phil Mag.*

Received 31 December 1973 and accepted 1 March 1974.